Reduced sodium channel density, altered voltage dependence of inactivation, and increased susceptibility to seizures in mice lacking sodium channel β2-subunits

Chunling Chen*†, Vandana Bharucha*†‡, Yuan Chen†§, Ruth E. Westenbroek†§, Angus Brown¶‖, Jyoti Dhar Malhotra*, Dorothy Jones, Christy Avery*, Patrick J. Gillespie III††, Kristin A. Kazen-Gillespie*, Katie Kazarinova-Noyes‡‡, Peter Shrager‡‡, Thomas L. Saunders††, Robert L. Macdonald**§§, Bruce R. Ransom¶, Todd Scheuer§, William A. Catterall§¶¶, and Lori L. Isom*¶¶**

Departments of *Pharmacology and **Neurology, and ††Transgenic Animal Model Core Laboratory, University of Michigan, Ann Arbor, MI 48109; Departments of §Pharmacology and ¶Neurology, University of Washington, Seattle, WA 98195; and ‡‡Departments of Neurobiology/Anatomy and Biochemistry/Biophysics, University of Rochester Medical Center, Rochester, NY 14642

Contributed by William A. Catterall, October 21, 2002

Sodium channel β-subunits modulate channel gating, assembly, and cell surface expression in heterologous cell systems. We generated $\beta2^{-/-}$ mice to investigate the role of β2 in control of sodium channel density, localization, and function in neurons *in vivo*. Measurements of [^{3}H]saxitoxin (STX) binding showed a significant reduction in the level of plasma membrane sodium channels in $\beta2^{-/-}$ neurons. The loss of β2 resulted in negative shifts in the voltage dependence of inactivation as well as significant decreases in sodium current density in acutely dissociated hippocampal neurons. The integral of the compound action potential in optic nerve was significantly reduced, and the threshold for action potential generation was increased, indicating a reduction in the level of functional plasma membrane sodium channels. In contrast, the conduction velocity, the number and size of axons in the optic nerve, and the specific localization of $Na_v1.6$ channels in the nodes of Ranvier were unchanged. $\beta2^{-/-}$ mice displayed increased susceptibility to seizures, as indicated by reduced latency and threshold for pilocarpine-induced seizures, but seemed normal in other neurological tests. Our observations show that β2-subunits play an important role in the regulation of sodium channel density and function in neurons *in vivo* and are required for normal action potential generation and control of excitability.

auxiliary subunits | gene targeting | epilepsy | action potential conduction

Voltage-gated sodium channels in mammalian brain are composed of a central, pore-forming α-subunit and one or two β-subunits (1). Cloning and functional analysis of the β-subunits have implicated them in regulation of channel gating, assembly, and cell surface expression (2–4). β-subunits are also involved in homophilic (5) and heterophilic (6) cell adhesion and in interactions with extracellular matrix and cell adhesion molecules (7–9), ankyrin (5, 9–11), and receptor tyrosine phosphatase-β (RPTPβ; ref. 12).

The effect of β2-subunits on cell surface expression of sodium channels is well established *in vitro* (13, 14). In primary neuronal cultures, newly synthesized α-subunits accumulate in the Golgi complex. These intracellular, "free" α-subunits are not disulfide-linked with β2. The appearance of channels at the cell surface is correlated with β2 association through disulfide bonds. Coexpression of α and β2 in oocytes increased sodium current density (15). Expression of β2 in the presence or absence of α resulted in the promotion of intracellular vesicular fusion with the membrane (15). Thus, β2 may be involved in translocation and immobilization of sodium channels in specific cell surface locations.

In the experiments described here, we used gene-targeting methods to investigate the role of β2-subunits in regulation of sodium channel density and function *in vivo*. Our results show that β2 plays an important role in determining sodium channel density and functional expression in neurons and in controlling electrical excitability in the brain.

Experimental Procedures

The experimental procedures for disruption of the gene encoding β2-subunits and for verification of the gene deletion and loss of β2 protein in $\beta2^{-/-}$ mice by Northern blot, Western blot, histology and immunocytochemistry of brain slices are presented in *Supporting Text*, which is published as supporting information on the PNAS web site, www.pnas.org.

[^{3}H]STX Binding. To measure STX binding to brain membranes, adult $\beta2^{+/+}$ and $\beta2^{-/-}$ mice were killed, and brains were immediately dissected on ice. Membranes were prepared, and [^{3}H]STX binding was measured as described (16) by using a vacuum filtration assay with 5 nM [^{3}H]STX (Amersham Pharmacia) and 10 μM tetrodotoxin (TTX, Calbiochem) to assess nonspecific binding. To measure STX binding to intact cultured brain neurons, mouse pups were killed by decapitation at postnatal day 1, and primary cultures were prepared in poly(D)-lysine-coated 6-well tissue culture dishes using the entire brain as described (14). The cultures were maintained for 21 days after treatment with fluorodeoxyuridine before analysis. [^{3}H]STX binding was performed on ice as described (16), except that binding was performed on attached cells in the culture dish.

Voltage-Clamp Analysis of Hippocampal Neurons. Hippocampal neurons from adult (>2 months old) mice were acutely isolated and analyzed by whole-cell voltage clamp by using standard procedures (17). The extracellular recording solution contained 20 mM NaCl, 10 mM Hepes, 1 mM $MgCl_2$, 1 mM $CdCl_2$, 60 mM CsCl, 150 mM glucose (pH 7.3, 300–305 mOsm/liter). The intracellular solution contained: 189 mM *N*-methyl D-glucamine,

†C.C., V.B., Y.C., and R.E.W. contributed equally to this work.

‡Present address: King Faisal Hospital Children's Cancer Centre, MBC 98-16, Riyadh, Kingdom of Saudi Arabia 11211.

‖Present address: Applied Neurosciences Group, University of Nottingham, Queens Medical Centre, Nottingham NG7 2UH, United Kingdom.

§§Present address: Department of Neurology, School of Medicine, Vanderbilt University, Nashville, TN 37212.

¶¶To whom correspondence should be addressed. E-mail: wcatt@u.washington.edu or lisom@umich.edu.

www.pnas.org/cgi/doi/10.1073/pnas.212638099

40 mM Hepes, 4 mM $MgCl_2$, 0.1 mM BAPTA, 0.1 mM NaCl, 25 mM phosphocreatine, 2 mM ATP, 0.2 mM GTP, 0.1 mM leupeptin (pH 7.2, 270–275 mOsm/liter). Electrode resistances were typically 3–5 MΩ in the bath. Series resistance was 80% compensated, and current was filtered at 10 kHz. Normalized conductance-voltage and inactivation-voltage curves were fit with a Boltzmann relationship, $1/\{1 + \exp[(V-V_{0.5})/k]\}$, where V was the depolarization voltage, $V_{0.5}$ was the half activation (V_a) or inactivation (V_h) voltage, and k was a slope factor.

Action Potential Conduction in Optic Nerve. Compound action potentials in optic nerves were measured as described (18). For 40 mM Na^+ experiments, 113 mM choline chloride was substituted for an equal concentration of NaCl.

Immunocytochemistry of Nerve Axons. Sciatic nerve sections were rinsed, fixed, and rinsed again as described (18) and blocked by using 5% normal goat serum and 5% nonfat milk for 1 h. The sections then were incubated in anti-β2-ec antibody, goat anti-rabbit IgG, and avidin D-fluorescein diluted in TBS containing 5% nonfat milk and 5% normal goat serum. The slides then were rinsed and coverslipped as described (18) and viewed by using the confocal microscope. Optic nerves were removed fresh from adult mice, desheathed, treated with collagenase (3.5 mg/ml) for 15 min, rinsed, and then teased apart on a slide containing Cell-Tak (Becton Dickinson). The slides were rinsed (18) and double-labeled with anti-$Na_v1.2$ (Chemicon, diluted 1:25) and anti-pan sodium channel (Sigma, diluted 1:50) or anti-$Na_v1.6$ (Chemicon, diluted 1:25) and anti-pan sodium channel overnight at room temperature with the above blocking agent. The slides then were rinsed again (18), incubated in biotinylated goat anti-rabbit IgG (diluted 1:300) and anti-mouse IgG-Texas red (Vector, diluted 1:100) for 2 h, rinsed, and incubated in avidin D-fluorescein (diluted 1:300) and anti-mouse IgG-Texas red (diluted 1:100) for 2 h at room temperature. The slides then were rinsed and prepared for viewing (18).

Demyelination/Remyelination. $\beta2^{-/-}$ mice and their $\beta2^{+/+}$ control littermates were anaesthetized with fentanyl-droperidol, and sciatic nerves were demyelinated by exposure to lysolecithin as described (19). On the experiment day, the animal was killed by CO_2 asphyxiation and the sciatic nerve was dissected, desheathed, and dissociated into single fibers with collagenase/dispase (3.5 mg/ml). Axons were teased over coverslips coated with drops of Cell-Tak and fixed in 4% (wt/vol) paraformaldehyde in 0.1 M phosphate buffer, pH 7.4 (PB) for 30 min. Alternatively, in some preparations, nerves were fixed before teasing; results were identical in both procedures. Optic nerves were dissected and fixed in 4% (wt/vol) paraformaldehyde in PB at room temperature for 10 min, then postfixed in 100% methanol at 4°C for 10 min and washed in PB for 10 min. The tissue was cryoprotected, frozen in OCT compound, and cut into 15-μm sections. All preparations were permeabilized in PB containing 0.3% Triton X-100 and 10% (vol/vol) goat serum (PBTGS). Washes and antibody dilutions also were made in PBTGS. Primary antibodies against myelin associated glycoprotein (MAG), pan sodium channels, and Caspr have been described (19–22). Secondary antibodies were coupled to Cy-3 (Accurate Scientific, Westbury, NY), Alexa-488 (Molecular Probes), or AMCA (Accurate Scientific). Fibers were observed under a Nikon Microphot fluorescence microscope fitted with a Hamamatsu C4742–95 cooled charge-coupled device video camera, and images were analyzed by using Image-Pro (Media Cybernetics, Silver Spring, MD).

Pilocarpine Induced Seizures in WT and $\beta2^{-/-}$ Mice. Prolonged seizures were induced in $\beta2^{+/+}$ and $\beta2^{-/-}$ mice of both sexes (25–40 g) by i.p. injection of pilocarpine (340 mg/kg, Sigma).

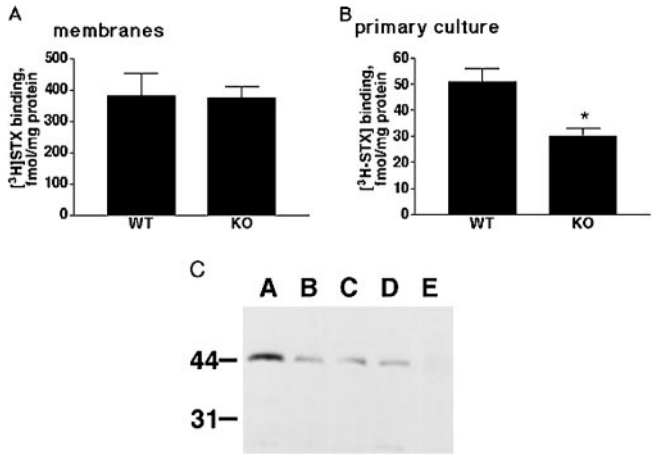

Fig. 1. [3H]STX-binding analysis of membrane preparations and primary cultured neurons from $\beta2^{+/+}$ and $\beta2^{-/-}$ mice. (*A*) Specific [3H]STX binding to brain membranes from $\beta2^{+/+}$ and $\beta2^{-/-}$ mice. Error bars show SEM. (*B*) Specific [3H]STX binding to primary cultures from $\beta2^{+/+}$ and $\beta2^{-/-}$ mouse brains. Error bars show SEM; *, $P = 0.0245$. (*C*) Western blot analysis. Lane A, rat brain membranes; lane B, neurons from $\beta2^{+/+}$ mouse B326; lane C, neurons from $\beta2^{+/+}$ mouse B392; lane D, neurons from $\beta2^{+/+}$ mouse B368; lane E, neurons from $\beta2^{-/-}$ mouse A10.

Scopolamine methylnitrate (1 mg/kg, Sigma) was administered via i.p. injection 30 min before the pilocarpine injection to limit peripheral cholinergic effects. Control animals were injected with scopolamine methylnitrate and the same volume of H_2O instead of pilocarpine. Seizures were characterized by facial automatisms, forelimb clonus, rearing, and falling. Seizures were quantified by using the classification of Racine *et al.* (23); animals were classified as having seizures if a stage 3 seizure (forelimb clonus) or higher was observed.

Results and Discussion

β2-Null Mutant Mice. The β2 gene was disrupted by homologous recombination, and heterozygous $\beta2^{+/-}$ mice and two lines of homozygous $\beta2^{-/-}$ mice (C10 and H5) were analyzed as described in *Supporting Text*. Except where noted below, all experiments described here compared F_2 hybrid mice (+/+; control) to F_2 hybrid littermate heterozygotes (+/−) and homozygotes (−/−). β2 mRNA and protein were significantly reduced in $\beta2^{+/-}$ and were not detected in $\beta2^{-/-}$ mice. β1-subunits were not up-regulated in brains of $\beta2^{-/-}$ mice. Brain development was grossly normal in $\beta2^{-/-}$ mice. Immunocytochemical studies of $\beta2^{+/+}$ mice revealed β2-subunits in many regions of the nervous system, including the nodes of Ranvier of sciatic nerve, the cell bodies of hippocampal and cortical pyramidal neurons, the cerebellar Purkinje neurons, and the nodes of Ranvier in white matter tracts in the cerebellum. No specific staining for β2-subunits was observed in these regions in $\beta2^{-/-}$ mice. These results indicate that deletion of the β2 protein was essentially complete in $\beta2^{-/-}$ mice.

Sodium Channel Density in $\beta2^{-/-}$ Mice. We measured specific binding of the membrane-impermeant probe [3H]STX in brain membrane preparations to assess total sodium channels and in neuronal primary cultures to measure cell surface sodium channels (14). We observed approximately equal [3H]STX binding in membrane preparations from adult $\beta2^{+/+}$ and $\beta2^{-/-}$ mouse brains (Fig. 1*A*, 380 ± 73 fmol/mg, SEM, $n = 5$ vs. 372 ± 39, SEM, $n = 7$). In contrast, we observed a 42% reduction in the number of plasma membrane sodium channels in primary cultures from $\beta2^{-/-}$ mice (51 ± 5 fmol/mg, SEM, $n = 3$ vs. 30 ± 3 fmol/mg, SEM, $n = 3$; $P = 0.0245$; Fig. 1*B*). Western blot

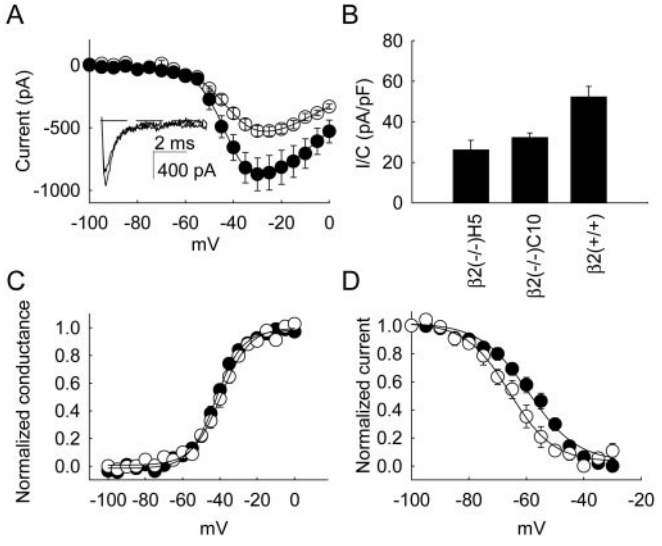

Fig. 2. Sodium currents in acutely dissociated hippocampal neurons from $\beta2^{-/-}$ mice. (*A*) Mean current-voltage relationships for $\beta2^{+/+}$ (●) and $\beta2^{-/-}$ (○) mice from a holding potential of −80 mV normalized to the peak current and averaged ($\beta2^{+/+}$, $n = 12$; $\beta2^{-/-}$, $n = 10$). (*Inset*) Example current traces at −10 mV from $\beta2^{+/+}$ (larger) and $\beta2^{-/-}$ (smaller) mice. (*B*) Mean peak sodium current was measured at the minimum of the current–voltage relationship (−25 to −30 mV) and normalized to cell capacitance from neurons dissociated from $\beta2^{+/+}$ ($n = 12$ cells from six mice), $\beta2^{-/-}$ H5 ($n = 8$ cells from three mice), and $\beta2^{-/-}$ C10 ($n = 11$ cells from six mice) lines. Cell capacitance did not differ between groups. (*C*) Mean conductance-voltage relationships. Conductance-voltage data from individual experiments were fit with a Boltzmann relationship (see *Experimental Procedures*). For $\beta2^{-/-}$ C10 cells, $V_a = -41.0 \pm 1.6$ mV, $k = 6.95 \pm 0.47$ mV ($n = 10$); for $\beta2^{+/+}$, $V_a = -42.3 \pm 1.27$ mV, $k = 6.36 \pm 0.39$ mV ($n = 8$). (*D*) Steady-state inactivation of sodium currents in $\beta2^{+/+}$ and $\beta2^{-/-}$ neurons. The average half inactivation voltage for $\beta2^{-/-}$ C10 neurons was -67.5 ± 2.78 mV, $k = 7.22 \pm 0.90$ mV ($n = 10$), and for $\beta2^{+/+}$ neurons, it was -56.9 ± 2.46, $k = 8.25 \pm 0.72$ mV ($n = 10$; $P < 0.01$).

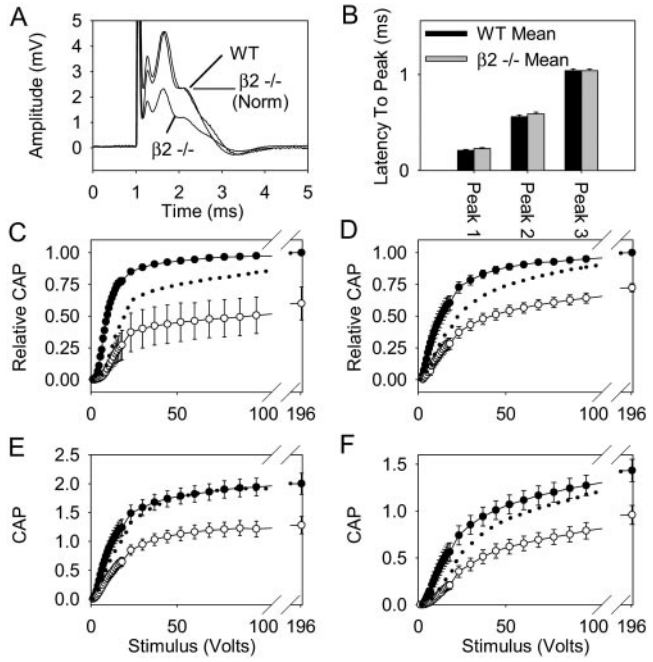

Fig. 3. Reduced sodium current in optic nerves of $\beta2^{-/-}$ mice. (*A*) Compound action potentials for $\beta2^{+/+}$, $\beta2^{-/-}$, and normalized $\beta2^{-/-}$. (*B*) Latency from stimulus to action potential recording for each peak in the compound action potential. (*C–F*) The areas of optic nerve compound action potentials are plotted as a function of stimulus intensity. (*C*) $\beta2^{+/+}$ in 140 mM Na^+: ●, control; ○, 10 nM TTX; ••••, 10 nM TTX normalized ($n = 3$). (*D*) $\beta2^{+/+}$: ●, control; ○, 40 mM Na^+; ••••, 40 mM Na^+ normalized ($n = 16$). (Bars = 1 mV, 0.5 ms.) (*E*) ●, $\beta2^{+/+}$, 140 mM Na^+ ($n = 16$); ○, $\beta2^{-/-}$ C10, 140 mM Na^+; ••••, $\beta2^{-/-}$ C10 normalized ($n = 16$). (*F*) ●, $\beta2^{+/+}$, 40 mM Na^+ ($n = 16$); ○, $\beta2^{-/-}$ C10, 40 mM Na^+; ••••, $\beta2^{-/-}$ C10 normalized ($n = 16$). CAP, compound action potential area in mV/ms.

analysis showed that β2 polypeptides were expressed at the time of the binding experiments in $\beta2^{+/+}$ cultures but not in $\beta2^{-/-}$ cultures (Fig. 1*C*). Thus, the absence of β2-subunits caused a decrease in plasma membrane sodium channels in intact neurons in cell culture.

Functional Properties of Sodium Channels in $\beta2^{-/-}$ Mice. We studied sodium currents in acutely isolated hippocampal neurons from $\beta2^{+/+}$ and $\beta2^{-/-}$ mice by whole-cell recording. The maximal amplitude of the sodium current was significantly reduced in both C10 and H5 $\beta2^{-/-}$ lines compared with $\beta2^{+/+}$ (Fig. 2 *A* and *B*; $P < 0.01$, ANOVA), and the voltage dependence of inactivation was negatively shifted by 10.6 mV (Fig. 2*D*; $P < 0.01$). No change was observed in the kinetics of activation or inactivation (Fig. 2*A Inset*) or in the voltage dependence of activation of the sodium current (Fig. 2*C*).

The negative shift in the voltage dependence of inactivation in hippocampal neurons from $\beta2^{-/-}$ mice implies that β2-subunits shift the voltage dependence of inactivation positively *in vivo*. Previous studies have shown that coexpression of β2-subunits with α-subunits in heterologous cells causes a negative shift in the voltage dependence of inactivation in *Xenopus* oocytes (15) but a positive shift in the voltage dependence of inactivation in human embryonic kidney cells (24). Evidently, the cell background has an important influence on the effect of β-subunits on steady-state inactivation of sodium channels, presumably caused by differential modulation of sodium channel function by intracellular second messenger processes. Our results show that the positive shift in the voltage dependence of inactivation observed in human embryonic kidney cells most closely resembles the effect of β2-subunits in hippocampal neurons.

Because steady-state inactivation was negatively shifted in $\beta2^{-/-}$ mice, we measured peak sodium currents at holding potentials of −80 mV (in 20 mM Na^+) and −100 mV (in 10 mM Na^+ with NaCl replaced by 20 mM glucose) to test whether the reduction of peak sodium current was caused by the shift in the voltage dependence of inactivation. The reduction in peak sodium current was observed clearly at each potential, which is consistent with the conclusion that the density of functional sodium channels is indeed reduced in hippocampal neurons from $\beta2^{-/-}$ mice. This result is in good agreement with the reduction in [^{3}H]STX binding in primary cultures of neurons from $\beta2^{-/-}$ mice.

Reduction of Sodium Current Density but Not Conduction Velocity in Optic Nerves of $\beta2^{-/-}$ Mice. We tested whether sodium currents were also reduced in the optic nerve by using the two-suction-electrode technique to record the compound action potential, which is characterized by three peaks corresponding to fibers having three different conduction velocities (Fig. 3*A*; refs. 18 and 25). To determine how a 50% reduction in sodium current would affect the compound action potential, we applied 10 nM TTX, approximately equal to its K_D, and generated compound action potentials as a function of stimulus intensity (Fig. 3*C*). The areas of normalized compound action potentials were reduced to 0.60 ± 0.11 of control values ($P < 0.01$). As compound action potential area is proportional to local circuit currents (25), this result is consistent with 10 nM TTX reducing compound action potential current by 40%. Similarly,

reduction of extracellular Na^+ from 140 mM to 40 mM decreased the normalized compound action potential area to 0.72 ± 0.03 (Fig. 3*D*). TTX and low Na^+ also altered the dependence of compound action potential area on stimulus intensity (Fig. 3 *C* and *D*) such that the threshold (rheobase) for action potential generation occurred at a higher stimulus voltage, and the compound action potential area grew less steeply as a function of voltage. Evidently, reduction in sodium current causes both a reduction in compound action potential area and a shift of the compound action potential vs. voltage curve to higher stimulus voltages.

We applied the same protocols to $\beta2^{+/+}$ and $\beta2^{-/-}$ mice to determine the effect of the null mutation on sodium current in the optic nerve. Compound action potential area at maximal stimulation (196 V) was reduced to 64% of its initial value, from 2.00 ± 0.18 mV·ms ($n = 16$) in $\beta2^{+/+}$ mice to 1.28 ± 0.15 mV·ms ($n = 16$; $P < 0.01$) in $\beta2^{-/-}$ mice (Fig. 3*C*). In 40 mM Na^+, compound action potential area was reduced to 67% of its initial value, from 1.43 ± 0.11 mV·ms in $\beta2^{+/+}$ to 0.96 ± 0.10 mV·ms in $\beta2^{-/-}$ mice ($n = 16$; $P < 0.01$; Fig. 3*D*). These results are consistent with a 30–40% reduction of sodium current in optic nerves. Changes in the voltage dependence of compound action potential area were also apparent in the $\beta2^{-/-}$ mice. Compound action potential area increased more slowly with voltage in $\beta2^{-/-}$ mice at 140 mM Na^+ (Fig. 3*E*), and this effect was more striking at 40 mM Na^+ (Fig. 3*F*). Thus, both the reduction in area of the compound action potential and the positive shift of threshold indicate reduced sodium current at the nodes of Ranvier from $\beta2^{-/-}$ mice.

To examine the effect of deletion of $\beta2$ on action potential propagation, we measured the temporal latency from the stimulus to time of recording of the three peaks of the compound action potential (25). The latency was unchanged between $\beta2^{+/+}$ and $\beta2^{-/-}$ mice, indicating that conduction velocity was unchanged (Fig. 3*B*). In contrast, we observed a significant increase in latency, indicating that the conduction velocity is measurably decreased, by reducing the number of functional sodium channels by ≈50% by application of TTX (10 nM). The reduction of Na^+ current in the $\beta2^{-/-}$ mice may be smaller in magnitude than for WT in 10 mM TTX, or conduction of a fraction of nerve fibers may be completely blocked in $\beta2^{-/-}$ mice, resulting in a distribution of conduction velocities similar to WT. Alternatively, compensatory changes in axonal or nodal structure or resistance may mask the effect of the reduced number of sodium channels on conduction velocity in the $\beta2^{-/-}$ mice.

Normal Fiber Number and Sodium Channel Localization in Myelinated Axons of $\beta2^{-/-}$ Mice. The reduction of sodium current in optic nerves in $\beta2^{-/-}$ mice might reflect a specific effect of the $\beta2$-subunit on functional expression of sodium channels, or it might indicate that there are fewer or smaller axons in the nerves from the $\beta2^{-/-}$ mice, abnormal localization of sodium channels in those axons, or substitution of a different sodium channel in the $\beta2^{-/-}$ nodes. To measure number and diameter of nerve fibers, optic nerves were cut in cross-section, and the axons were labeled by using antineurofilament antibodies. Confocal images were randomly collected along the length of the optic nerve, and the number of axons per image was counted and sized with the METAMORPH image analysis program. The average number of axons was 521 axons per image in $\beta2^{+/+}$ mice ($n = 20$) vs. 519 axons per image in $\beta2^{-/-}$ mice ($n = 20$). No change in the size distribution of axons was detected.

To assess the structure of the nodes of Ranvier in the $\beta2^{-/-}$ mice, the distribution of molecular constituents of the nodes and adjacent paranodes was examined through immunocytochemistry. In sciatic nerve, sodium channels were properly clustered in the nodal gap, and MAG was present at high density in the myelinating Schwann cells, especially at the paranodes (Fig. 4*A*). During remyelination of sciatic nerve, sodium channels clustered at the tips of Caspr-positive Schwann cell processes (Fig. 4*B*, *sing*) formed binary structures as Schwann cells extended processes longitudinally, an intermediate step in node formation (Fig. 4*B*, *bin*; ref. 19), and became highly focal as the binary clusters fused (Fig. 4*B*, *focal*). There were no obvious differences in the timing or appearance of these sites between $\beta2^{-/-}$ and $\beta2^{+/+}$ mice. Similarly, sodium channels in optic nerve axons were present at high density in the nodal gap, and Caspr was clustered in the adjacent paranodes, as expected (Fig. 4*C*).

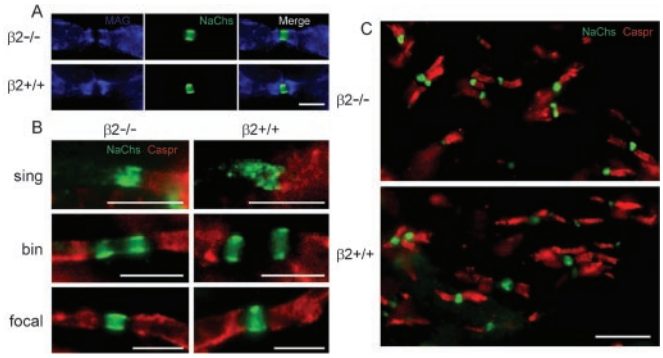

Fig. 4. Sodium channel clustering and node of Ranvier formation in $\beta2^{-/-}$ mice. Blue, MAG; green, sodium channels; red, Caspr. (*A*) Nodes of Ranvier in adult sciatic axons from $\beta2^{-/-}$ and $\beta2^{+/+}$ mice. (*B*) Sodium channel clustering and formation of new nodes of Ranvier during remyelination, 14 days after injection. sing, single Schwann cell processes and associated sodium channel clusters; bin, binary sets of clusters; focal, new nodes with focal clusters of sodium channels. (*C*) Nodes of Ranvier in adult optic nerves of $\beta2^{+/+}$ and $\beta2^{-/-}$ mutant mice. [Bars = 5 μm (*A* and *B*); 10 μm (*C*).]

Changes in sodium current density and properties might also arise if a different sodium channel α-subunit was present in the nodes of Ranvier. Normally, in rat nerves, $Na_v1.2$ channels are present early in development, but after myelination, the primary sodium channel in adult nodes of Ranvier is $Na_v1.6$ (26–28). Adult optic nerves from both $\beta2^{+/+}$ and $\beta2^{-/-}$ mice do contain $Na_v1.6$ (Fig. 5 *A–F*) but not $Na_v1.2$ (Fig. 5 *G–L*). These findings confirm that $Na_v1.6$ is present at nodes of Ranvier of both $\beta2^{-/-}$ and $\beta2^{+/+}$ mice.

Differential Susceptibility to Seizures Induced by i.p. Injection of Pilocarpine. Visual observations of $\beta2^{-/-}$ mice showed that they are normal in size, weight, posture, and gait. Their righting reflex and eye blink reflex are normal. They also performed normally in the rotarod test of motor coordination and were able to learn the rotarod test normally. These general tests of neurological function indicate that there is no broad impairment of nervous system function.

In contrast, we found that the $\beta2^{-/-}$ mice are prone to epileptic seizures. Behaviorally observed seizures were induced in 25- to 40-g F_2 generation $\beta2^{+/+}$ and $\beta2^{-/-}$ mice by using i.p. injections of 340 mg/kg pilocarpine preceded 30 min by scopolamine methylnitrate. Although stage 3 seizures were provoked in both strains, $\beta2^{-/-}$ mice were significantly more susceptible to the convulsant effects of pilocarpine. In WT animals, only 7 of 12 (58%) animals developed seizures, whereas in the $\beta2^{-/-}$ mice, 13 of 14 (93%) animals developed seizures (Fig. 6*A*; $P < 0.05$, χ^2 analyses). In addition, there was a significantly shortened latency to stage 3 seizures in the $\beta2^{-/-}$ mice. WT mice developed stage 3 seizures in 29.9 ± 3.5 min (mean ± SEM), whereas the $\beta2^{-/-}$ mice progressed to stage 3 seizures in 17.9 ± 2.4 min (Fig. 6*B*; $P < 0.05$, Student's *t* test).

To confirm that this difference in seizure susceptibility was

NEUROSCIENCE

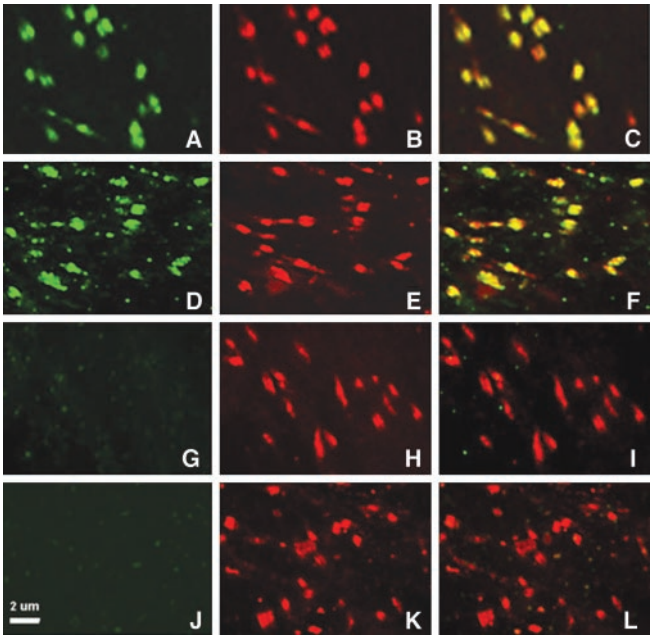

Fig. 5. Localization of $Na_v1.2$ and $Na_v1.6$ in optic nerves from $\beta2^{-/-}$ mice. (*A–C*) Optic nerve fibers from $\beta2^{-/-}$ mice double-labeled with anti-Nav1.6 (*A*) and anti-pan sodium channel (*B*) antibodies illustrating colocalization of these antibodies at the nodes of Ranvier of optic nerves (*C*). Regions of overlap are shown in yellow and yellow/orange. (*D–F*) Optic nerve fibers from $\beta2^{+/+}$ mice double-labeled with anti-$Na_v1.6$ (*D*) and anti-pan sodium channel (*E*) illustrating colocalization (*F*) of these antibodies in the optic nerve. (*G–I*) Optic nerve fibers from $\beta2^{+/+}$ mice double-labeled with anti-$Na_v1.2$ (*G*) and anti-pan sodium channel (*H*) antibodies. Regions of overlap would appear yellow in the merged image (*I*). (*J–L*) Optic nerves from $\beta2^{-/-}$ mice double-labeled with anti-$Na_v1.2$ (*G*) and anti-pan sodium channel (*H*) antibodies. Regions of overlap would appear yellow in the merged image (*L*).

caused by deletion of $\beta2$, we also analyzed N_{10} generation mice bred into the C57BL/6J background, which are less susceptible to seizures induced by pilocarpine. In this more homogeneous genetic background, the difference in seizure susceptibility was even more striking (Fig. 6*C*). All $\beta2^{-/-}$ mutant mice had seizures after pilocarpine injection, whereas only 20% of $\beta2^{+/+}$ mice were affected ($P < 0.01$, χ^2 test). Considering the normal neurological profile of these mice, this seizure susceptibility phenotype is a highly specific finding, suggesting impairment *in vivo* of their regulation of excitability.

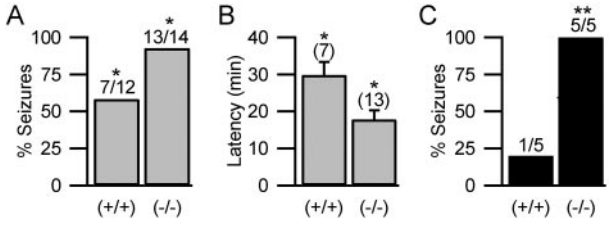

Fig. 6. Pilocarpine-induced stage 3 seizures in WT and $\beta2^{-/-}$ mice. (*A*) The frequency of prolonged seizures induced by 340 mg/kg pilocarpine was different in F_2 hybrid $\beta2^{+/+}$ and $\beta2^{-/-}$ mice. The $\beta2^{-/-}$ mice exhibited an increased frequency of stage 3 (forelimb clonus) or higher seizure activity compared with $\beta2^{+/+}$ mice (*, $P < 0.05$, χ^2 analyses). (*B*) Latency to onset of pilocarpine-induced stage 3 seizures in F_2 hybrid $\beta2^{+/+}$ and $\beta2^{-/-}$ mice. The latency to stage 3 seizures induced by 340 mg/kg pilocarpine was different in $\beta2^{+/+}$ and $\beta2^{-/-}$ mice. The $\beta2^{-/-}$ mice had a decreased latency to stage 3 seizures compared with $\beta2^{+/+}$ mice (*, $P < 0.05$, Student's *t* test). The number of mice tested is shown above each bar. (*C*) Seizure frequency after injection of 340 mg/kg of pilocarpine as in *A* for N_{10} generation mice in the C57BL/6J genetic background. (Bars represent SEM.) **, $P < 0.01$.

In humans, it has been shown that generalized epilepsy with febrile seizures (GEFS + 1), a juvenile form of epilepsy that persists beyond 6 yr of age, involves a loss-of-function mutation in the voltage-gated sodium channel $\beta1$-subunit gene (SCN1B; ref. 29). Although the $\beta2$-subunit has not been identified as a major genetic contributor to common idiopathic generalized epilepsies (30), it may have a more indirect role in contributing to individual susceptibility to development of epilepsy in humans.

The most likely mechanism for increased seizure susceptibility of the $\beta2^{-/-}$ mice with reduced sodium channel expression is reduced excitability of inhibitory interneurons. They may be more affected by the deletion of $\beta2$-subunits because they have a lower margin of safety for action potential generation or a greater decrease in sodium channel density than excitatory neurons. In either case, deletion of the $\beta2$-subunit would reduce inhibitory tone and favor hyperexcitability in neural circuits of downstream excitatory neurons that are disinhibited. This interpretation of our results is supported by pharmacological studies of local anesthetics, which are nonselective blockers of sodium channels. Entry of local anesthetics into the brain results in a general reduction in sodium current, which leads to clonic seizures. A selective depression of inhibitory neurons is thought to account for this excitatory phase of toxicity *in vivo* (31), so a general reduction of sodium current should result in a hyperexcitable phenotype, as observed in the $\beta2^{-/-}$ mice. Thus, there is a close correlation between the reduction in sodium current density observed at the cellular level in hippocampal neurons and in myelinated nerves and the increased susceptibility to seizures observed in the $\beta2^{-/-}$ mice.

Functions of $\beta2$-Subunits *in Vivo*. Sodium channel β-subunits are multifunctional. Like the auxiliary subunits of voltage-gated calcium and potassium channels, they modulate gating and voltage dependence as well as regulate expression in the plasma membrane (3). Unlike these other auxiliary subunits, sodium channel β-subunits are cell adhesion molecules of the Ig superfamily, which interact with extracellular matrix, transmembrane signaling, and cell adhesion molecules (5–12). We show here that $\beta2$-subunits have essential roles *in vivo* in maintenance of normal electrical excitability of neurons. They are not required for sodium channel expression or for life, as the $\beta2^{-/-}$ mice seem to develop normally, have normal brain, axon, and neuronal morphology, as well as normal neurological function, and live typical life spans. However, $\beta2$-subunits are required for normal voltage dependence of inactivation of sodium currents and for maintenance of the normal level of sodium channels at the plasma membrane in neuronal cell bodies and in myelinated axons. These $\beta2$-dependent defects in electrical excitability at the cellular level lead to hyperexcitability and a reduced threshold for seizures, probably because of reduced excitability of inhibitory interneurons. Thus, normal control of sodium channel function and expression and of neuronal excitability requires $\beta2$-subunits.

We thank Richard Mulligan for the pPNT plasmid, Andras Nagy, Reka Nagy, and Wanda Abramow-Newerly for the R1 ES cells, and Mr. Matthew Koopmann, Ms. Payel Gupta, Ms. Ann Yen, and Ms. Thuy Vien for expert technical assistance. We thank Drs. Bruce Tempel and Neil Nathanson for comments on a draft of the manuscript. This project was supported by National Multiple Sclerosis Society Research Grant RG-2882-A-1 (to L.L.I. and W.A.C.), National Science Foundation Research Grant IBN-9734462 (to L.L.I.), National Institutes of Health Research Grants NS25704 (to W.A.C.), R01 NS39479 (to R.L.M.), NIMH 5T32 MH 19547 (to D.J.), and NS17965 (to P.S.), and University of Michigan Grants 5P30CA46592, 3P60DK20572-22S2, 5P30DK34933, and 5T32HD07505-03. J.D.M. was supported by a National Multiple Sclerosis Society postdoctoral fellowship.

1. Catterall, W. A. (2000) *Neuron* **26,** 13–25.
2. Goldin, A. L. (1993) *Curr. Opin. Neurobiol.* **3,** 272–277.
3. Isom, L. L., De Jongh, K. S. & Catterall, W. A. (1994) *Neuron* **12,** 1183–1194.
4. Isom, L. L. (2000) *Am. J. Physiol.* **278,** G349–G353.
5. Malhotra, J. D., Kazen-Gillespie, K., Hortsch, M. & Isom, L. L. (2000) *J. Biol. Chem.* **275,** 11383–11388.
6. Kazarinova-Noyes, K., Malhotra, J. D., McEwen, D. P., Mattei, L. N., Berglund, E. O., Ranscht, B., Levinson, S. R., Schachner, M., Shrager, P., Isom, L. L. & Xiao, Z.-C. (2001) *J. Neurosci.* **21,** 7517–7525.
7. Ratcliffe, C. F., Westenbroek, R. E., Curtis, R. & Catterall, W. A. (2001) *J. Cell Biol.* **154,** 427–434.
8. Srinivasan, J., Schachner, M. & Catterall, W. A. (1998) *Proc. Natl. Acad. Sci. USA* **95,** 15753–15757.
9. Xiao, Z.-C., Ragsdale, D. S., Malhorta, J. D., Mattei, L. N., Braun, P. E., Schachner, M. & Isom, L. L. (1999) *J. Biol. Chem.* **274,** 26511–26517.
10. Srinivasan, Y., Elmer, L., Davis, J., Bennett, V. & Angelides, K. (1988) *Nature* **333,** 177–180.
11. Malhotra, J. D., Koopmann, M. C., Kazen-Gillespie, K. A., Hortsch, M. & Isom, L. L. (2002) *J. Biol. Chem.* **277,** 26681–26688.
12. Ratcliffe, C. F., Qu, Y., McCormick, K. A., Tibbs, V. C., Dixon, J. E., Scheuer, T. & Catterall, W. A. (2000) *Nat. Neurosci.* **3,** 437–444.
13. Schmidt, J., Rossie, S. & Catterall, W. A. (1985) *Proc. Natl. Acad. Sci. USA* **82,** 4847–4851.
14. Schmidt, J. W. & Catterall, W. A. (1986) *Cell* **46,** 437–445.
15. Isom, L. L., Ragsdale, D. S., De Jongh, K. S., Westenbroek, R. E., Reber, B. F., Scheuer, T. & Catterall, W. A. (1995) *Cell* **83,** 433–442.
16. Isom, L. L., Scheuer, T., Brownstein, A. B., Ragsdale, D. S., Murphy, B. J. & Catterall, W. A. (1995) *J. Biol. Chem.* **270,** 3306–3312.
17. Cantrell, A. R., Ma, J. Y., Scheuer, T. & Catterall, W. A. (1996) *Neuron* **16,** 1019–1026.
18. Brown, A. M., Westenbroek, R. E., Catterall, W. A. & Ransom, B. R. (2001) *J. Neurophysiol.* **85,** 900–911.
19. Dugandzija-Novakovic, S., Koszowski, A. G., Levinson, S. R. & Shrager, P. (1995) *J. Neurosci.* **15,** 492–503.
20. Rasband, M. N., Peles, E., Trimmer, J. S., Levinson, S. R., Lux, S. E. & Shrager, P. (1999) *J. Neurosci.* **19,** 7516–7528.
21. Peles, E., Nativ, M., Lustig, M., Grumet, M., Schilling, J., Martinez, R., Plowman, G. D. & Schlessinger, J. (1997) *EMBO J.* **16,** 978–988.
22. Poltorak, M., Sadoul, R., Keilhauer, G., Landa, C., Fahrig, T. & Schachner, M. (1987) *J. Cell Biol.* **105,** 1893–1899.
23. Racine, R. J. (1972) *Electroencephalogr. Clin. Neurophysiol.* **32,** 281–294.
24. Qu, Y., Curtis, R., Lawson, D., Gilbride, K., Ge, P., DiStefano, P. S., Silos-Santiago, I., Catterall, W. A. & Scheuer, T. (2001) *Mol. Cell. Neurosci.* **18,** 570–580.
25. Stys, P. K., Ransom, B. R. & Waxman, S. G. (1991) *Brain Res.* **546,** 18–32.
26. Caldwell, J. H., Schaller, K. L., Lasher, R. S., Peles, E. & Levinson, S. R. (2000) *Proc. Natl. Acad. Sci. USA* **97,** 5616–5620.
27. Kaplan, M. R., Cho, M.-H., Ullian, E. M., Isom, L. L., Levinson, S. R. & Barres, B. A. (2001) *Neuron* **30,** 105–119.
28. Boiko, T., Rasband, M., Levinson, S., Caldwell, J., Mandel, G., Trimmer, J. & Matthews, G. (2001) *Neuron* **30,** 91–104.
29. Wallace, R. H., Wang, D. W., Singh, R., Scheffer, I. E., George, A. L., Jr., Phillips, H. A., Saar, K., Reis, A., Johnson, E. W., Sutherland, G. R., *et al.* (1998) *Nat. Genet.* **19,** 366–370.
30. Haug, K., Sander, T. & Hallman, K. (2000) *NeuroReport* **11,** 2687–2689.
31. Catterall, W. A. & Mackie, K. (1996) in *Goodman and Gilman's The Pharmacological Basis of Therapeutics*, eds. Hardman, J. G. & Limbird, L. E. (McGraw–Hill, New York), pp. 331–347.